

- β_1 = volumetric expansion coefficient
 Γ = gamma function
 θ_m = dimensionless bulk mean temperature
 θ_h = dimensionless temperature function for horizontal systems
 θ_v = dimensionless temperature function for vertical systems
 ν = kinematic viscosity
 ρ = density
 ρ_0 = reference density
 ψ = dimensionless stream function

LITERATURE CITED

1. Berman, A. S., *J. Appl. Phys.*, **24**, 1232 (1953).
2. Carter, L. F., and W. N. Gill, *A.I.Ch.E. J.*, **10**, 330 (1964).
3. Eckert, E. R. G., P. L. Donoughe, and B. J. Moore, *Natl. Advisory Comm. Aeronaut. Tech. Note 4102* (1957).
4. Gill, W. N., *Appl. Sci. Res.*, **A11**, 10 (1962).
5. Mercer, A. McD., *Appl. Sci. Res.*, **A8**, 357 (1959), **A9**, 450 (1960).
6. Morgan, G. W., and W. H. Warner, *J. Aeronaut. Sci.*, **23**, 937 (1956).
7. Rao, A. K., *Appl. Sci. Res.*, **A11**, 1 (1962).

Manuscript received July 19, 1965; revision received October 4, 1965; paper accepted October 6, 1965.

Simultaneous Axial Dispersion and Adsorption in a Packed Bed

RAUL CHAO and H. E. HOELSCHER

Johns Hopkins University, Baltimore, Maryland

A study has been made of simultaneous axial dispersion and solid-fluid mass exchange in a packed-bed adsorber. Four different and mutually exclusive controlling mechanisms for the solid-fluid mass exchange rate are considered. A dimensionless parameter K characterizes this interphase mass transfer. The Peclet number characterizes axial dispersion.

An impulse-response technique was used to obtain simultaneously values of the axial Peclet number and the rate parameter K in the adsorption column. Values of the Peclet number obtained under conditions of interphase mass transfer were found to be significantly smaller than the values measured under pure mixing (no surface activity) conditions.

The mathematical model used to analyze the results includes the particular case of no surface activity with results previously found from the dispersion model. One result not previously derived from the dispersion model was found and tested experimentally.

Recently, considerable attention has been focussed on systems in which chemical processes as well as heat and/or mass transfer take place simultaneously. A complete description of such systems is available for only the simplest geometries, but an increased interest in transport phenomena in, for example, beds of porous solids, is more than justified by the demand for more rigorous design of catalytic reactors, chromatographic and ion exchange columns, beds of adsorbents, etc.

The design of a catalytic reactor must be based on the continuity, energy, and momentum equations coupled by a common term containing the reaction rate. A frontal approach to this set of differential equations remains prohibitively and hopelessly complicated. It is recognized,

however, that an understanding of those problems which involve only mass transfer serves as a basis for an understanding of similar problems which are complicated by the presence of chemical reactions. Thus adsorbent beds or chromatographic columns are the natural precursors of packed bed reactors for studies of dynamic responses of the latter.

In any such study, one must consider mixing processes, interfacial mass transfer, surface and pore diffusion, and adsorption processes as well as the chemical reactions that may occur.

Analyses of longitudinal and radial interparticle diffusion by Aris and Amundson (3), Carberry and Bretton (7), McHenry and Wilhelm (23), and Wehner and Wilhelm (25) have grown into a vast literature, mostly utilizing a dispersion model (diffusion type of equation with a diffusivitylike coefficient). These efforts, however,

Raul Chao is with Esso Research and Engineering Company, Florham Park, New Jersey. H. E. Hoelscher is at the University of Pittsburgh, Pittsburgh, Pennsylvania.

have considered only mixing processes, excluding surface activity and mass exchange between the solid surface and the fluid phase.

Film diffusion has also been the object of considerable work since the new classical papers of Gamson, Thodos, and Hougen (13, 29).

Acivos (1), Amundson and Lapidus (20), Klinkenberg (18), Deisler and Wilhelm (12), Wicke (27, 28), Wheeler (26), and others (16, 17, 12, 14) have studied intraparticle and surface diffusion but, as with most studies on solid-fluid exchange processes, the effect of external diffusion or bulk gas phase mixing on these phenomena has received little attention or has been neglected altogether. A recent review of such studies by Vermeulen (24) and a comprehensive bibliography on reaction engineering by Hoelscher (15) can be found elsewhere.

The primary purpose of this present work was to study longitudinal dispersion in a packed bed in which a surface exchange process was occurring. The extent to which mass transfer at an active particle surface affects the mixing pattern in an adsorption column or a chemical reactor had not previously been determined. The parameter characterizing axial dispersion in such a system (the Peclet number) has heretofore been measured without mass exchange at or on the surface. It was the further purpose of this work to devise a method for measuring this dispersion process in the presence of such a surface exchange process.

The experimental procedure involved an impulse-response study. Such techniques were introduced in 1953 by Zwietering (30, 31) and Dankwerts (10) to determine the extent of mixing, that is, the degree of departure from pistonicity in flow reactors. Since then, they have been reviewed many times (7, 11) and such a review will therefore not be included here. A brief review of such functions of the residence-time distributions as to the moments and their usefulness in the analysis of systems has been presented by Levenspiel (21).

The mathematical model chosen for this present work is basically the dispersion model used so extensively for mixing studies with an extra term to account for the mass

exchange at an active surface. Bischoff and Levenspiel (5) have presented a complete review of the use of this model by other investigators.

EXPERIMENTAL EQUIPMENT AND PROCEDURE

Equipment

The experimental studies were carried out in a packed-bed reactor consisting of five 1-in. I.D. by 6-in. long brass working sections and one straightening section of the same dimensions. Figure 1 is a schematic of this experimental apparatus. A pulse generator was placed between the working and the straightening sections. Its main features include a sliding compartment that can suddenly be placed in line with the reactor, thus introducing a "slug" of gases of known composition into the working section. Further details are available elsewhere (8).

Since this study called for both active and inert solid surfaces, two types of packing material were used. For the mixing runs, the reactor was packed with broken glass chips; for adsorption studies it was packed with active charcoal particles, their dimensions being the same as the glass chips. The average particle diameter was 0.1 in. in both cases. The active material used was the equivalent of the Pittsburgh Activated Carbon Company No. 281-1621 with a B.E.T. surface area of approximately 800 sq. meters/g.

Gas flow and composition were controlled and measured with standard rotameters. Pressure was regulated both before and after the rotameters. Factory calibrations of rotameters were checked by water displacement. Built-in thermal conductivity cells were placed inside the reactor after the first working section and before the last one. The analytical section of the reactor was thus limited to 18 in. in length. This 18-in. long section between the two analytical probes shall be called the reactor in the mathematical development that will follow. It is an open vessel reactor in the terminology of Levenspiel (21).

The design of the built-in thermal conductivity probe is shown in Figure 2. The resistor on the probe was a 0.002 in. O.D. platinum wire threaded in a hexagonal arrangement through nineteen thermal conductivity cells in series. The design of the probe was such that their signals gave an average

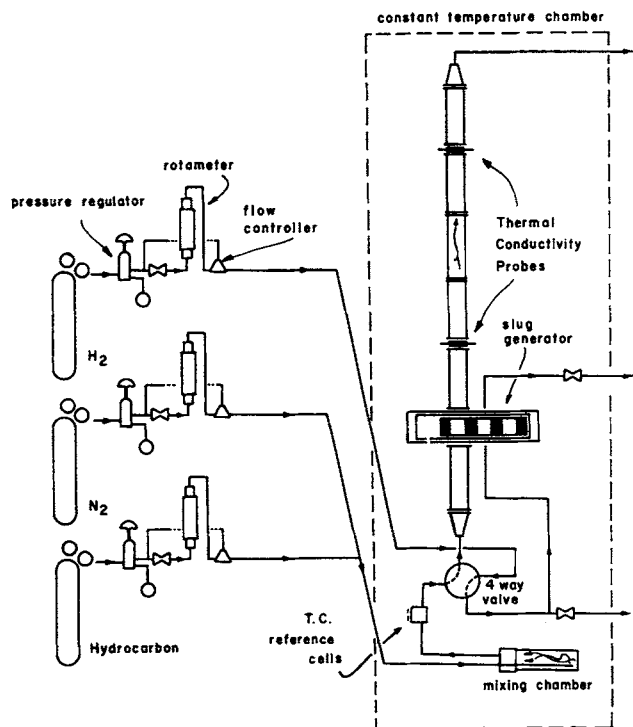


Fig. 1. Experimental apparatus.

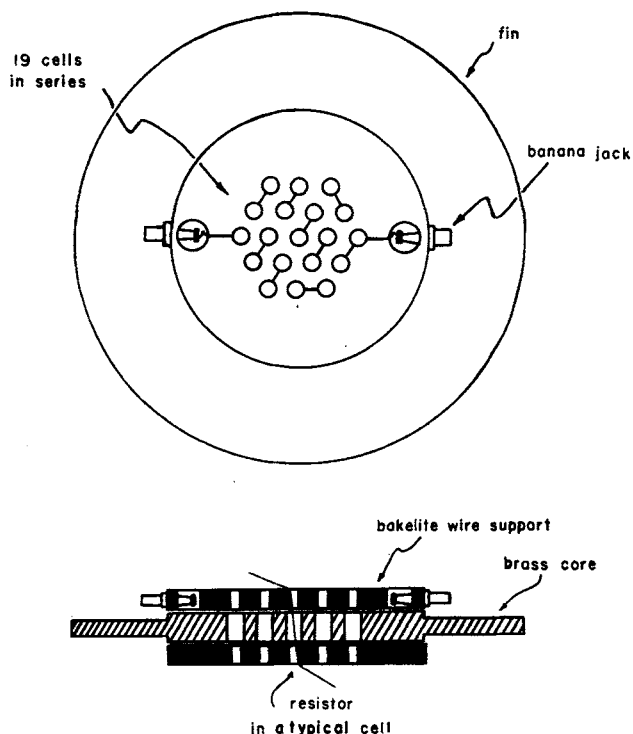


Fig. 2. Thermal conductivity probes.

composition over the cross section of the reactor. The core of the thermal conductivity cells was made of brass and the wire-supporting disks were bakelite. The total resistance of the probes was 27 ohms. Since they were placed directly on-stream, their response was very fast. The reference cells for these probes were two Gow-Mac thermal conductivity cells (9,225 mounts, tungsten) with resistances near those of the probes. They were located upstream from the reactor.

The electrical circuit was similar to that generally used in chromatography. The signals from the two detecting stations were recorded by two separate Minneapolis-Honeywell high speed recorders with a span step response time rating of 0.25 sec., a chart speed of 1 in./sec., and a 0 to 1 mv. range.

The reactor, the mixing chamber for the carrier gases, and the thermal conductivity reference cells were all enclosed in a well-insulated 5 cu. ft. constant temperature air chamber controlled within $\pm 0.1^\circ\text{C}$. by means of a Bimetal thermostat and a supersensitive relay.

Procedure

The experiments described below were all carried out at room temperature. Prior to a run, a mixture of nitrogen and one of the hydrocarbons was passed through the entire reactor until thermal equilibrium was established, that is, until a stable base line was observed at both recording stations. During this time, hydrogen was passed through the off-line section of the pulse generator.

A run was started when the slug of hydrogen was suddenly introduced in line by a quick movement of the slug generator slide. Provisions were made to start both recorder charts simultaneously by a single switch. Time zero was taken in both recordings as the point where the pressure pulse (the disturbance in the recorder base line due to the introduction of a gas sample in the column) was noted.

Each run was repeated three times to check reproducibility of the recorded signals. Before the next run was made, ample time (usually less than 25 min.) was allowed for the reactor to reach equilibrium with a new carrier gas composition. Reproducibility of the recorded signals was taken as a criterion for carrier gas-solid surface equilibrium during a run. An independent chemical analysis of the pulse as it emerged from the reactor was performed for two different carrier gas compositions, since there was some doubt as to whether the recorded signals were indeed hydrogen waves traveling along the reactor, or if they were, in part, hydrocarbon ejected from the surface by an irreversible adsorption of the hydrogen pulse introduced at the inlet of the reactor. The analysis clearly showed that there was not an increase of hydrogen concentration in or around the recorded pulse and that the pulse itself was hydrogen. The analysis for hydrocarbon is thought to have been sensitive to within $\pm 5\%$. The details of this analysis are presented elsewhere (8).

From each run two pieces of information were obtained, namely, the hydrogen concentration history at the two detecting positions along the reactor. The difference in the time means between these two pulses was the mean residence time of the hydrogen pulse in the section of the reactor comprised between the two detecting stations. It gave an independent check on the carrier gas flow rates for the mixing runs.

From the recorded hydrogen pulses, readings were made and the moments around the mean and area under the curve were obtained by an IBM 7094 computer.

Three sets of runs were made in the course of this study. Each set consisted of between nine and eleven runs with a carrier gas of varying hydrocarbon composition (0 to 100%) for both inert (glass) and active (charcoal) packing material. The hydrocarbons used were ethylene, propylene, and butene-1. The pulse was pure hydrogen in all three sets.

The flow rate used throughout the work varied from 3.46 to 3.59 cu.ft./hr. The steady state average residence time varied from 8.15 to 8.25 sec. The average linear velocity varied from 0.176 to 0.183 ft./sec. The void fraction in the bed was 0.425 throughout all runs.

MATHEMATICAL TREATMENT

The system under consideration is a packed column through which a gas of known composition is flowing. The

surface concentration of gases adsorbed thereon is in a dynamic equilibrium with the gas phase. At some point near the inlet a pulse of tracer gas (hydrogen), which can be adsorbed and/or desorbed at the solid surface, is introduced. At two points downstream the tracer concentration history in time is recorded.

A material balance on the tracer, taken over a differential section of the column yields

$$D \frac{\partial^2 c}{\partial x^2} - v \frac{\partial c}{\partial x} - \frac{\partial c}{\partial t} - \frac{1}{\alpha} \frac{\partial w}{\partial t} = 0 \quad (1)$$

To solve Equation (1) the rate of the adsorption process must be related to the concentration of active material in the fluid phase.

It may be shown (8) that such an expression can be written in the following form for at least four surface mechanisms, any one of which may control the overall rate process:

$$\frac{1}{\alpha} \frac{\partial w}{\partial t} = \frac{1}{R} (c - c^*) \quad (2)$$

The equilibrium concentration c^* must be related to the adsorbate concentration at the surface w . It is assumed that, for low tracer concentrations, a linear isotherm can be used, that is

$$w = B c^* \quad (3)$$

Equation (2) then takes the form

$$\frac{1}{\alpha} \frac{\partial w}{\partial t} = \frac{1}{R} \left(c - \frac{w}{B} \right) \quad (4)$$

The following dimensionless variables are now defined:

$$\begin{aligned} y &= x/L & \theta &= vt/L \\ N_{Pe} &= vL/D^\dagger & q &= c/c_o \\ K &= Rv/L & W &= w/w_o \end{aligned}$$

Equations (1) and (4) become

$$\frac{1}{N_{Pe}} \frac{\partial^2 q}{\partial y^2} - \frac{\partial q}{\partial y} - \frac{\partial q}{\partial \theta} - \frac{w_o}{\alpha c_o} \frac{\partial W}{\partial \theta} = 0 \quad (5)$$

$$\frac{W_o}{\alpha c_o} \frac{\partial W}{\partial \theta} = \frac{1}{K} q - \frac{w_o L}{RBvc_o} W \quad (6)$$

The boundary conditions for Equations (5) and (6) are

$$\begin{aligned} W(y, 0) &= 0 \\ q(y, 0) &= 0 \\ q(0, \theta) &= F(\theta) \end{aligned} \quad (7)$$

The first of these boundary conditions states that no adsorbed material is present in the bed at time zero. The second states that no active species are present in the fluid phase at time zero. The third says that at $y = 0$ (bed entrance) the tracer concentration is a well-defined and known function of time.

Equations (5) and (6) are now reduced to a single equation by the methods of operational mathematics and, in particular, the Laplace transformation. Both equations are transformed with respect to the time variable θ and $\bar{w}(y, s)$, the solid phase concentration of adsorbed species in transformed space, is eliminated from the resulting equations. These operations yield

$$\frac{1}{N_{Pe}} \bar{q}_{yy} - \bar{q}_y - \bar{q} h = 0 \quad (8)$$

[†] $N_{Pe} = vL/D$ is defined here solely for convenience. The standard definition $N_{Pe} = vD_p/D$ is used throughout the remainder of the text and in presenting all data and results.

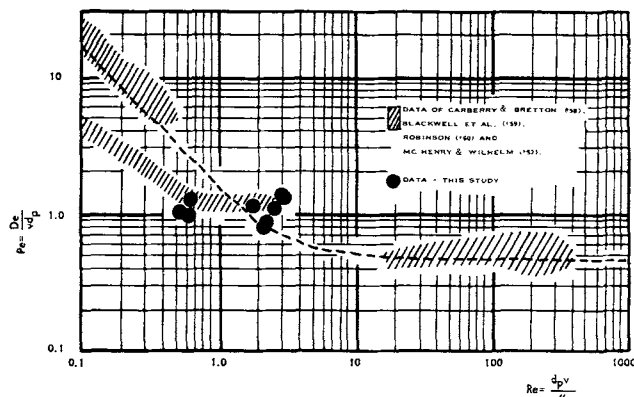


Fig. 3. Results for the pure mixing runs.

where

$$\bar{q}_{yy} = \frac{\partial^2}{\partial y^2} \bar{q}(y, s)$$

$$h = s + \frac{LB}{RBvs + \alpha L} \quad (9)$$

Equation (8) is solved with the boundary conditions in transformed space, that is

$$\bar{q}(y, 0) = 0$$

$$\bar{q}(0, s) = \bar{F}(s)$$

$$\lim_{y \rightarrow \infty} \bar{q}(y, s) = \text{finite}$$

The Laplace transformation of the original boundary conditions is discussed in some detail elsewhere (8).

These boundary conditions give the solution of Equation (8) as

$$\bar{q}(y, s) = \bar{F}(s) e^{by} e^{-ny} \quad (10)$$

where

$$b = \frac{N_{Pe}}{2} \quad (10a)$$

$$n = \sqrt{b^2 + h N_{Pe}} \quad (10b)$$

This solution (10) satisfies the condition for the conservation of mass, that is

$$\lim_{s \rightarrow 0} \bar{q}(y, s) = \text{constant}$$

since

$$\lim_{s \rightarrow 0} h(s) = 0$$

$$\lim_{h \rightarrow 0} n(h) = b$$

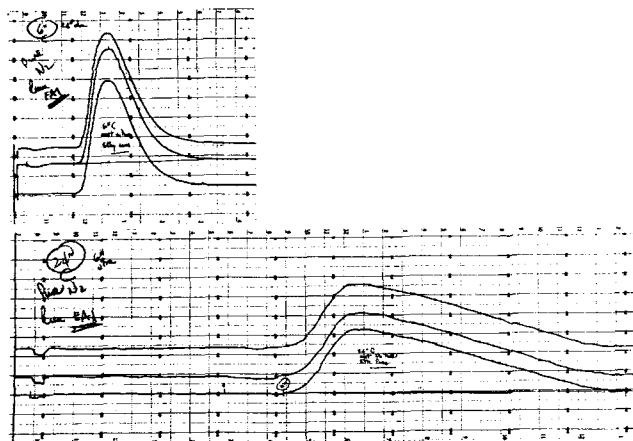


Fig. 4. Photographs of recordings. Run EA 1.

From (10), using the operational properties of the Laplace transform (9), namely

$$\int_0^\infty \theta^n q(y, \theta) d\theta = (-1)^n \lim_{s \rightarrow 0} \frac{\partial^n}{\partial s^n} q(y, s)$$

we arrive at the following equations:

$$\mu(y) = y \lim_{s \rightarrow 0} \frac{dn}{ds} \quad (11)$$

$$\sigma^2(y) = \sigma_i^2 - y \lim_{s \rightarrow 0} \left[\frac{d^2n}{ds^2} - y \left(\frac{dn}{ds} \right)^2 \right] \quad (12)$$

$$\pi^3(y) = \pi_i^3 + \lim_{s \rightarrow 0} \left[y \frac{d^3n}{ds^3} - 3y^2 \frac{dn}{ds} \frac{d^2n}{ds^2} + y^3 \left(\frac{dn}{ds} \right)^3 + 3y \sigma_i^2 \frac{dn}{ds} \right] \quad (13)$$

where

$$\mu(y) = \int_0^\infty \theta q(y, \theta) d\theta$$

$$\sigma^2(y) = \int_0^\infty \theta^2 q(y, \theta) d\theta$$

$$\pi^3(y) = \int_0^\infty \theta^3 q(y, \theta) d\theta$$

It is more convenient to express the second and third moments around the mean of the distribution (its first moment). To do so, use is made of the following equations:

$$\int_0^\infty (\theta - \mu)^2 q(y, \theta) d\theta = \int_0^\infty \theta^2 q(y, \theta) d\theta - \mu^2 \quad (14)$$

$$\int_0^\infty (\theta - \mu)^3 q(y, \theta) d\theta = \int_0^\infty \theta^3 q(y, \theta) d\theta - 3\mu \int_0^\infty \theta^2 q(y, \theta) d\theta + 2\mu^3 \quad (15)$$

With the help of (14) and (15), the equations for the first three moments (11), (12), and (13) are reduced to

$$\Delta\mu = \lim_{s \rightarrow 0} \frac{dn}{ds} \quad (16)$$

$$\Delta\sigma^2 = - \lim_{s \rightarrow 0} \frac{d^2n}{ds^2} \quad (17)$$

$$\Delta\pi^3 = \lim_{s \rightarrow 0} \frac{d^3n}{ds^3} \quad (18)$$

where the Δ 's refer to the difference in the moments between positions 2 ($y = 1$) and 1 ($y = 0$) along the column.

From Equations (10b), (10a), and (9) the following equations result:

$$\lim_{s \rightarrow 0} \frac{dn}{ds} = 1 + \frac{B}{\alpha} \quad (19)$$

$$\lim_{s \rightarrow 0} \frac{d^2n}{ds^2} = -2 \left(\frac{B}{\alpha} \right)^2 K - \frac{2}{N_{Pe}} \left(1 + \frac{B}{\alpha} \right)^2 \quad (20)$$

$$\lim_{s \rightarrow 0} \frac{d^3n}{ds^3} = 6 \left(\frac{B}{\alpha} \right)^3 K^2 + \frac{12}{N_{Pe}^2} \left(1 + \frac{B}{\alpha} \right)^3 + \frac{12}{N_{Pe}} \left(\frac{B}{\alpha} \right)^2 \left(1 + \frac{B}{\alpha} \right) K \quad (21)$$

TABLE 1. READINGS FROM RECORDINGS OF PULSE RUN EA1

Recording No. 1				Recording No. 2			
t_i	C_i	t_i	C_i	t_i	C_i	t_i	C_i
0	0	6.2	0.16	0	0	10.33	1.7
0.2	0.02	6.6	0.1	0.33	0.02	11.0	1.5
0.6	1.0	7.0	0.04	1.0	0.2	11.67	1.35
1.0	3.7	7.4	0	1.67	0.7	12.33	1.1
1.4	5.5			2.33	1.5	13.0	0.9
1.8	5.85	$(OP)_1 = 2.4$		3.0	2.52	13.67	0.7
2.2	5.45			3.67	3.18	14.33	0.5
2.6	4.5			4.33	3.24	15.0	0.37
3.0	3.45			5.0	3.2	15.67	0.2
3.4	2.5			5.67	3.05	16.33	0.1
3.8	1.7			6.33	2.8	17.0	0.03
4.2	1.15			7.0	2.64	17.33	0
4.6	0.8			7.67	2.47		
5.0	0.52			8.33	2.3	$(OP)_2 = 13.05$	
5.4	0.32			9.0	2.12		
5.8	0.22			9.67	1.9		

Combining these with (16), (17), and (18), one obtains the following:

$$\mu = 1 + \frac{B}{\alpha} \quad (22)$$

$$\Delta\bar{\sigma}^2 = 2(\mu - 1)^2 K + \frac{2}{N_{Pe}} \mu^2 \quad (23)$$

$$\Delta\bar{\pi}^3 = 6(\mu - 1)^3 K^2 + \frac{12}{N_{Pe}} \mu^3 + \frac{12}{N_{Pe}} (\mu - 1)^2 \mu K \quad (24)$$

Note that if no adsorption or mass exchange takes place at the surface, Equation (22) reduces to $\mu = 1$, which indicates that the center of mass of the pulse travels at the interstitial velocity, a result readily obtained from the dispersion model equations.

Under the same conditions (no mass exchange, $B = 0$) Equation (23) reduces to

$$\Delta\bar{\sigma}^2 = \frac{2}{N_{Pe}}$$

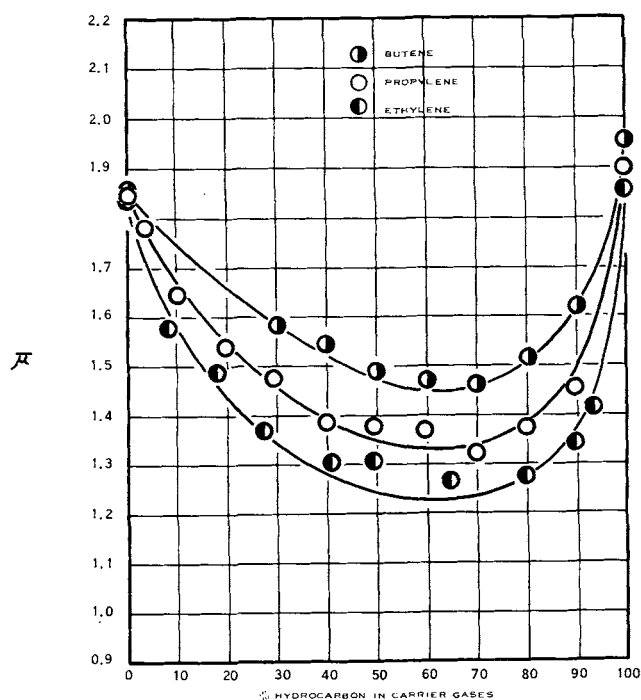


Fig. 5. Results from adsorption studies. Mean residence time of pulses.

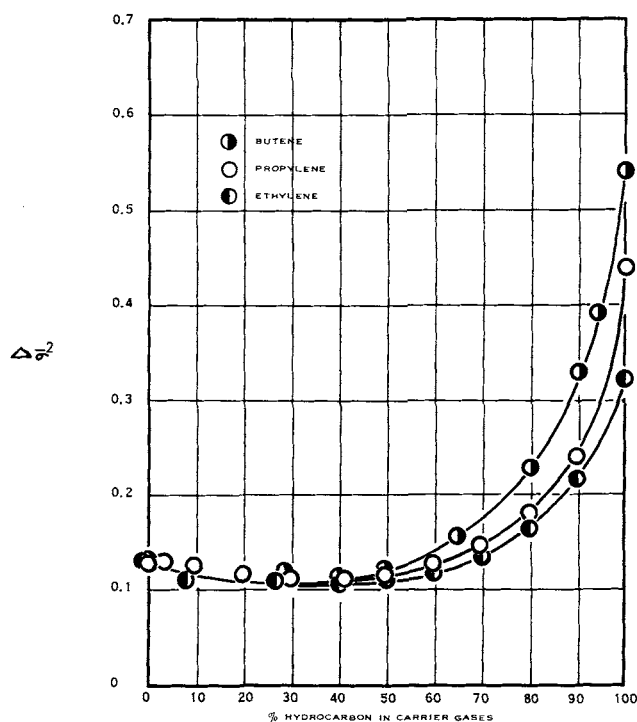


Fig. 6. Results from adsorption studies. Variance of pulses.

which is a well-known result (2) and Equation (24) reduces to

$$\Delta\bar{\pi}^3 = \frac{12}{N_{Pe}^2}$$

a result not previously reported in the literature.

Equations (22), (23), and (24) can be used to extract information on both the longitudinal dispersivity and the mass transfer process in a packed column from a single experiment.

DISCUSSION OF RESULTS

Two kinds of results were obtained during the course of this work: (1) results from studies using the packed bed as a mixer, that is with an inert packing; (2) results from the packed bed as an adsorption column, that is, with an active packing.

Helium and nitrogen were used as carrier gases during the first studies. The bed lengths were 18 and 24 in. and the pulses were ethylene. Mixtures of nitrogen and ethylene, propylene, or butene were used as carrier gases during the second. The bed length was 18 in. and the pulse was always hydrogen.

The first part of the experimental program involved only well-known techniques and results. It was, nevertheless, included as part of the program, since it seemed desirable to compare axial dispersivities (expressed in terms of the Peclet number) under pure mixing conditions obtainable from the reactor built for this work with those obtained in earlier studies. These results were indeed found comparable with all previous work as summarized, for example, by Levenspiel (20). Details of this preliminary work (which served only as a preliminary testing and familiarization study) are available elsewhere (8). A typical set of results is shown in Figure 3 and is compared with existing literature values obtained under similar pure mixing conditions.

The adsorption studies were of more direct concern. The desired information was obtained from the moments of the pulse recorded at two points along the bed. Three sets of data were obtained from a constant bed length

(18 in.), a pulse of pure hydrogen, and a carrier gas of a nitrogen-olefin mixture having from 0 to 100% olefin. Ethylene, propylene, and butene-1 were used and the bed was always brought to equilibrium—saturated—with the carrier gas prior to admitting the hydrogen pulse.

The run number identifies the hydrocarbon present in the carrier gases, its concentration, and the sequence of the runs. *E*, *P*, and *B* denote ethylene, propylene, or butene; numbers 1 to 11 denote increasing concentrations of hydrocarbon. *A* to *K* give the order in which the experiments were made.

A photograph of the recordings obtained during run *EA1* is presented in Figure 4. All recordings are on file in the Department of Chemical Engineering, The Johns Hopkins University.

A tabulation of results from the recordings for run *EA1* is presented in Table 1. The moments are calculated and made dimensionless (8). The resulting values are tabulated elsewhere (8) and are shown in Figures 5, 6, and 7. The characteristic time is again chosen to be L/v , that is, the mean residence time of the pulse under pure mixing conditions. The total flow rate of carrier gases was constant within each set, therefore all the runs in each set have the same characteristic time.

From the three dimensionless moments of the pulse, the values of the three parameters characterizing axial dispersion (the Peclet number), solid-fluid mass exchange (dimensionless number K), and gas-solid equilibrium (B) are obtained. Recapitulating, the equations for these three moments in terms of the parameters are

$$\bar{\mu} = 1 + \frac{B}{\alpha}$$

$$\Delta\bar{\sigma}^2 = 2(\bar{\mu} - 1)^2 K + \frac{2}{N_{Pe}} \bar{\mu}^2$$

$$\Delta\bar{\pi}^3 = 6(\bar{\mu} - 1)^3 K^2 + \frac{12}{N_{Pe}^2} \bar{\mu}^3 + \frac{12}{N_{Pe}} (\bar{\mu} - 1)^2 \bar{\mu} K$$

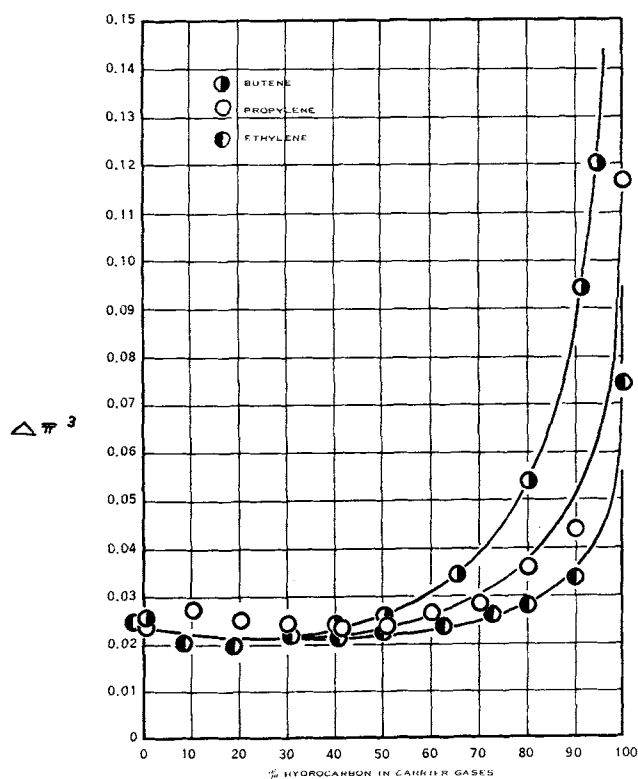


Fig. 7. Results from adsorption studies. Skewness of pulses.

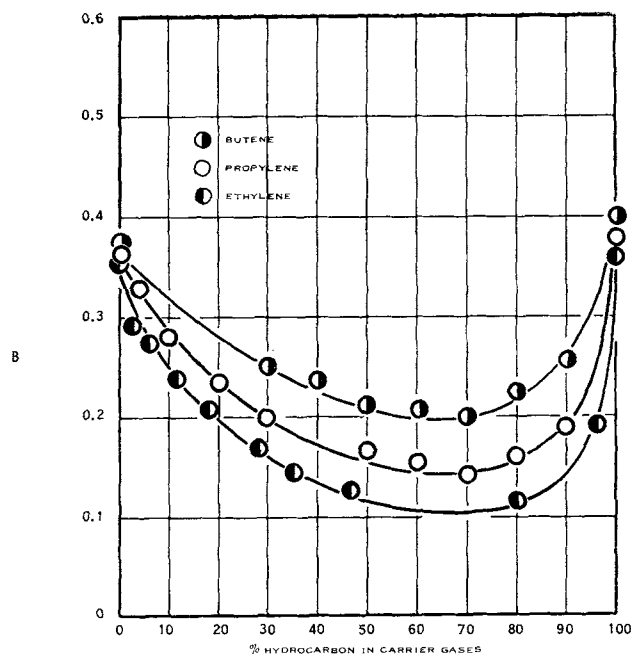


Fig. 8. Results from adsorption studies. Values of B .

B is readily obtained from the first equation. For example, the void fraction in the bed α , being 0.425, run *EA1* yields a value for B of 0.36. Values for the Peclet number and K are obtained from the last two equations once the values of $\Delta\bar{\sigma}^2$ and $\Delta\bar{\pi}^3$ are known. Again, for example, from the data of run *EA1*

$$\begin{aligned} \bar{\mu} &= 1.85 \\ \Delta\bar{\sigma}^2 &= 0.135 \\ \Delta\bar{\pi}^3 &= 0.028 \\ N_{Pe} &= 250 \text{ (based on bed length)} \\ N_{Pe} &= 1.39 \text{ (based on particle diameter)} \\ K &= 0.075 \end{aligned}$$

(For the present packed bed, L/d_p is 180. This was used to convert Peclet numbers based on bed length to Peclet numbers based on particle diameter.) Numerical values for B , K , and N_{Pe} for the runs in all three sets of adsorption experiments are available elsewhere (8). These values have been plotted against carrier gas concentrations of hydrocarbon in Figures 8, 9, and 10.

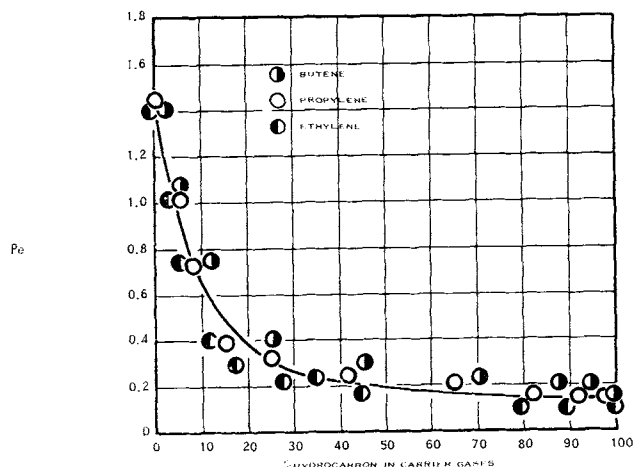


Fig. 9. Results of adsorption studies. Values of the Peclet number (Peclet number is based on particle diameter).

An order of magnitude analysis was made on the four resistances to mass transfer to be considered. The form of the resistance term in the mass transfer rate equation depends on the mechanism considered to control. The forms (8) are

$$R_{ED} = \frac{\rho B}{K_g a_v} \quad (\text{fluid phase external diffusion})$$

$$R_{PD} = \frac{\alpha r^2}{\pi^2 D_i B} \quad (\text{fluid phase pore diffusion})$$

$$R_{SD} = \frac{\alpha}{K_s a_v B} \quad (\text{surface diffusion})$$

$$R_R = \frac{\alpha}{k_r} \quad (\text{reaction, adsorption, or phase change})$$

For the packed bed used in the adsorption studies throughout this work, the following values of the variables involved are appropriate:

$$\begin{aligned} a_v &= 6/d_p \quad (\text{exact for spherical particles}) \\ K_g &= 0(10^{-5}) \text{ g./}(\text{sec.})(\text{sq. cm. conc.}) \\ d_p &= 0.04 \text{ cm.} = 0.1 \text{ in.} \\ D_i &= 0(10^{-5}) \text{ sq. cm./sec.} \\ K_s &= \text{very large (14)} \\ \rho B &= 0(1) \text{ g./cc.} \\ B &= 0(0.1) \\ L/v &= 0(10) \text{ sec.} \end{aligned}$$

Thus, order of magnitude of the resistance terms for the four possible controlling mechanisms are

$$\begin{aligned} R_{ED} &= 0(10^4) \\ R_{SD} &= 0(0.1/K_s) \\ R_{PD} &= 0(0.5) \\ R_R &= 0(0.5/k_r) \end{aligned}$$

The order of magnitude of the resistance term found experimentally in this present work was

$$\begin{aligned} R_{\max} &= (L/v) K_{\max} = 10(0.075) = 0(0.75) \\ R_{\min} &= (L/v) K_{\min} = 10(0.02) = 0(0.2) \end{aligned}$$

Experimental studies of surface diffusion (14) show K_s to be quite large, that is, $K_s \gg 1$. Thus, it seems reasonable to eliminate both fluid phase external diffusion and surface diffusion as possible controlling mechanisms in this work. Pore diffusion remains a possibility as does the surface kinetics, since nothing is known at present of k_r .

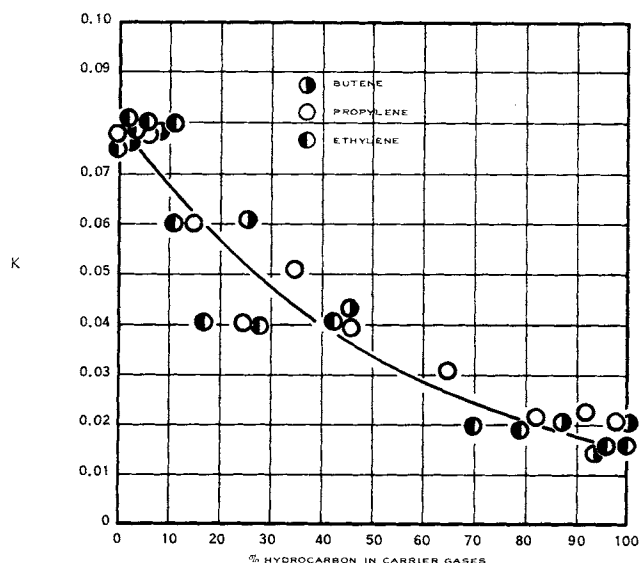


Fig. 10. Results from adsorption studies. Values of the constant K .

However, the value used for the internal diffusivity D_i in the calculation of R_{PD} is surely the lowest possible value for this quantity. If, as may be more likely, the value should properly be an order of magnitude greater, then the weight of evidence would indicate that the measured values of the constant K or R from this work relate to the kinetics of the adsorption process occurring on the solid surface. This observation requires further experimental verification before it can be advanced as a conclusion from this work.

CONCLUSIONS

The axial Peclet number obtained when there is a solid-fluid exchange process in the interphase was found to be generally smaller than that obtained under pure mixing conditions for the same Reynolds number. This may explain why packed-bed reactors frequently seem more stable than predicted (4), using values of the Peclet number from pure mixing studies. It now appears that mass transfer at the solid-fluid boundary decreases the value of the Peclet number, thus effectively increasing the values of the dispersion constant D and increasing the range of operating conditions permitting stable operation of the bed.

The order of magnitude analysis of the resistance term in the four mass transfer controlling mechanisms considered in the mathematical model makes it safe to exclude both fluid phase external diffusion and surface diffusion as the controlling mechanisms for the solid-fluid mass transfer. The order of magnitude for pore diffusional resistance seems to agree with the order of magnitude found experimentally for the resistance term in the mass transfer rate equation. On the other hand, no values of the adsorption rate constant k_r have been found in the literature and therefore the question of identifying the value of K found in this work with a pore diffusion mechanism or an adsorption rate controlling mechanism remains unanswered. Some insight into this question would be obtained if the methods of this present work were used to measure K at different reactor temperatures, since the temperature dependence of the pore diffusional resistance should be markedly different from the temperature dependence of the adsorption rate constant.

The values of B obtained in this present work depend exclusively on the mean residence time of the traveling pulse. There is some evidence for the linearity of the adsorption isotherm in the presence of a second adsorbate (6). The values of B obtained here can be related at least qualitatively to the equilibrium conditions at the solid-fluid interface for different hydrocarbon concentrations, but no claims can be made at this point that these values of B truly represent slopes of the hydrogen-charcoal isotherms.

The mathematical model and the frequency response technique proposed in this present work can be useful in the study of packed beds under conditions of simultaneous axial dispersion and solid-fluid mass transfer. The model proposed here, that is

$$D \frac{\partial^2 c}{\partial x^2} - v \frac{\partial c}{\partial x} - \frac{\partial c}{\partial t} - \frac{1}{\alpha} \frac{\partial w}{\partial t} = 0$$

$$\frac{1}{\alpha} \frac{\partial w}{\partial t} = \frac{1}{R} \left(c - \frac{w}{B} \right)$$

is a generalization of the dispersion model used to study mixing patterns in the fluid phase of packed columns. The equations previously obtained from the dispersion model arise in the above model as particular cases for no surface mass exchange conditions. An equation not previously obtained from the dispersion model has been theoretically

derived and experimentally verified by the results of the pure mixing studies in this work.

It seems evident from the results previously reported in the literature and from the results obtained in the course of this work that more data are required in the low Reynolds number range (0.1 to 100). This would indicate more precisely what effect, if any, the Schmidt number $\mu/\rho D$ has on the values of the dispersion number. Such a study is available at present for tubular flow and it seems to indicate that, for low values of the Reynolds numbers, there is a linear relationship between the Schmidt and the dispersion numbers (22).

ACKNOWLEDGMENT

The authors are sincerely grateful to the National Science Foundation for a research grant which supported the early stages of this work. To the Atomic Energy Commission, Chemistry Division, our thanks for support of the final stages of the study. We are deeply appreciative of the skilled workmanship of Bernard Baker who constructed much of the apparatus used throughout.

NOTATION

a_v	= external surface area of particles per unit volume of packed column
B	= slope of the adsorption isotherm
b	= $N_{Pe}/2$
c	= fluid phase concentration of active species
c^*	= fluid phase concentration of active species at the solid-fluid interface, presumably in equilibrium with the concentration of adsorbate in the solid surface
c_o	= reference concentration of tracer in the fluid phase
C_i	= concentration of tracer in the pulse
D	= dispersion coefficient in the dispersion model
D_t	= pore diffusion coefficient
d_p	= particle diameter
$F(\theta)$	= well-defined concentration vs. time function used as input in the frequency-response analysis
$\bar{F}(s)$	= the Laplace transform of $F(\theta)$
h	= function of s , defined in Equation (9)
K	= Rv/L
K_g	= fluid phase mass transfer coefficient
K_s	= solid or shell side mass transfer coefficient
k_r	= first-order rate constant for adsorption
L	= reactor length also Laplace transform operator
n	= function of h and N_{Pe} , defined in Equation (10b)
$(OP)_j$	= arbitrary zero point in recordings
N_{Pe}	= Peclet number = vd_p/D
q	= dimensionless concentration of tracer = c/c_o
q	= Laplace transformation of q
R	= resistance term in the mass transfer rate equation, defined in Equation (2)
r	= particle radius (sphere)
R_{ED}	= resistance term for fluid phase external diffusion
R_{PD}	= resistance term for fluid phase pore diffusion
R_{SD}	= resistance term for surface diffusion
R_R	= resistance term for adsorption
s	= Laplace transform variable
Sc	= Schmidt number = $\mu/\rho D$
t	= time
v	= interstitial velocity
W	= dimensionless concentration of adsorbed species on the solid phase = w/w_o
w	= concentration of adsorbed species on the solid surface
\bar{w}	= Laplace transform of w
w_o	= reference concentration of adsorbed species on the solid surface

x	= distance along the reactor
y	= dimensionless distance along the reactor = x/L

Greek Letters

α	= external void fraction
θ	= dimensionless time = vt/L
μ	= mean residence time of the pulse; also viscosity
σ^2	= variance of the pulse, that is, second moment around the mean
$\bar{\sigma}^2$	= dimensionless variance of the pulse
π^3	= skewness of the pulse, that is, third moment around the mean
$\bar{\pi}^3$	= dimensionless skewness of the pulse
ρ	= density
ρ_B	= bulk density of solids

Subscripts

y	= differentiation with respect to y
j	= detecting station
1,2	= detecting stations 1 and 2

LITERATURE CITED

1. Acrivos, A., *Chem. Eng. Sci.*, **13**, 1 (1960).
2. Aris, Rutherford, *ibid.*, **9**, 266 (1959).
3. ———, and N. R. Amundson, *A.I.Ch.E. J.*, **3**, 280 (1957).
4. Barkelew, C. H., *Chem. Eng. Progr. Symposium Ser. No. 25*, 55 (1957).
5. Bischoff, K. B., and O. Levenspiel, *Chem. Eng. Sci.*, **17**, 245 (1962).
6. Brunauer, S., "The Adsorption of Gases and Vapors," Princeton Univ. Press, N. J. (1945).
7. Carberry, J. J., and R. H. Bretton, *A.I.Ch.E. J.*, **4**, 367 (1958).
8. Chao, Raul, Ph.D. dissertation, Johns Hopkins Univ., Baltimore, Md. (1965).
9. Churchill, R. V., "Modern Operational Mathematics in Engineering," McGraw-Hill, New York and London (1944).
10. Danckwerts, P. V., *Chem. Eng. Sci.*, **2**, 1 (1953).
11. *Ibid.*, **8**, 93 (1958).
12. Deisler, P. F., and R. H. Wilhelm, *Ind. Eng. Chem.*, **45**, 1219 (1953).
13. Gamson, B. W., George Thodos, and O. A. Hougen, *Trans. A.I.Ch.E.*, **39**, 1 (1943).
14. Gilliland, E. R., et al., *A.I.Ch.E. J.*, **4**, 90 (1958).
15. Hoelscher, H. E., "Reaction Engineering, A Bibliography and Literature Guide," Am. Inst. Chem. Engrs., New York (1964).
16. Hougen, O. A., and W. R. Marshall, *Chem. Eng. Progr.*, **43**, 197 (1947).
17. Kasten, P. R., Leon Lapidus, and N. R. Amundson, *J. Am. Chem. Soc.*, **56**, 683 (1952).
18. Klinkenberg, A., J. J. van Deempter, and F. J. Zuiderweg, *Chem. Eng. Sci.*, **5**, 271 (1956).
19. Kramers, H., and G. Alberda, *ibid.*, **2**, 173 (1953).
20. Lapidus, Leon, and N. R. Amundson, *J. Phys. Chem.*, **56**, 948 (1952).
21. Levenspiel, O., "Chemical Reaction Engineering," Wiley, New York and London (1962).
22. ———, *Ind. Eng. Chem.*, **50**, 343 (1958).
23. McHenry, K. W., Jr., and R. H. Wilhelm, *A.I.Ch.E. J.*, **3**, 83 (1957).
24. Vermeulen, Theodore, in "Advances in Chemical Engineering," T. B. Drew, and J. W. Hoopes, ed., Vol. II, Academic Press, New York (1958).
25. Wehner, A., and R. H. Wilhelm, *Chem. Eng. Sci.*, **6**, 89 (1958).
26. Wheeler, A., in "Catalysis," P. H. Emmett, ed., Vol. II, Reinhold, New York (1955).
27. Wicke, E., *Kolloid Z.*, **86**, 167, 296 (1939).
28. *Ibid.*, **93**, 129 (1940).
29. Wilke, C. R., *Trans. A.I.Ch.E.*, **41**, 445 (1945).
30. Zwietering, Th. N., *Chem. Eng. Sci.*, **11**, 1 (1959).
31. *Ibid.*, **8**, 244 (1958).

Manuscript received March 25, 1965; revision received October 13, 1965; paper accepted October 18, 1965.